2015 IEEE International Conference on Robotics and Automation (ICRA)
Washington State Convention Center
Seattle, Washington, May 26-30, 2015

Towards Real-Time Under-Ice Acoustic Navigation at Mesoscale Ranges

Sarah E. Webster†, Lee E. Freitag*, Craig M. Lee†, Jason I. Gobat†

†Department of Ocean Physics
Applied Physics Laboratory, University of Washington
Seattle, WA, 98105, USA
swebster@apl.washington.edu
craig@apl.washington.edu
jgobat@apl.washington.edu

*Applied Ocean Physics Department
Woods Hole Oceanographic Institution
Woods Hole, MA, 24503, USA
lfreitag@whoi.edu

***Abstract*— This paper describes an acoustic navigation system that provides mesoscale coverage (hundreds of kilometers) under the ice and presents results from the first multi-month deployment in the Arctic. The hardware consists of ice-tethered acoustic navigation beacons transmitting at 900 Hz that broadcast their latitude and longitude plus several bytes of optional control data. The real-time under-ice navigation algorithm, based on a Kalman filter, uses time-of-flight measurements from these sources to simultaneously estimate vehicle position and depth-averaged local currents. The algorithm described herein was implemented on Seagliders, a type of autonomous underwater glider (AUG), but the underlying theory is applicable to other autonomous underwater vehicles (AUVs). As part of an extensive field campaign from March to September 2014, eleven acoustic sources and four Seagliders were deployed to monitor the seasonal melt of the marginal ice zone (MIZ) in the Beaufort and northern Chukchi Seas. Beacon-to-beacon performance was excellent due to a sound duct at 100 m depth where the transmitters were positioned; the travel-time error at 200 km has a standard deviation of 40 m when sound-speed is known, and ranges in excess of 400 km were obtained. Results with the Seagliders, which were not regularly within the duct, showed reliable acoustic ranges up to 100 km and more sparse but repeatable range measurements to over 400 km. Navigation results are reported for the real-time algorithm run in post-processing mode, using data from a 295-hour segment with significant time spent under ice.**

I. Introduction

Autonomous platforms have been used under the ice as early as the 1970's when Francois and Nodland deployed the Unmanned Arctic Research Submersible (UARS) in the Beaufort Sea [1]. Since then, numerous autonomous underwater vehicles (AUVs) and autonomous underwater gliders (AUGs) have successfully performed under-ice observations. These under-ice missions have pushed the limits of existing technology and provided highly valuable scientific information, but the ability for an autonomous platform to consistently estimate its own georeferenced position in real-time with acceptable accuracy remains a challenge [2], [3].

Currently, most AUGs and AUVs rely on fixed acoustic sources for vehicle-based navigation, or, in the case of mobile sources, the position estimation is performed on-board the ship or on a basestation. Seaglider AUGs were first deployed under the ice in Davis Strait in 2006 and have continued to be deployed routinely since then, relying on moored RAFOS acoustic navigation sources [4], [5]. The Slocum AUGs also have ice-capable behaviors and routinely operate at the ice edge in Antarctica [6]. For AUVs, the most commonly used under-ice navigation strategy is a combination of long baseline (LBL) navigation for its range and ultra-short baseline (USBL) navigation for its precision during homing maneuvers. Examples of this can be seen in the Odyssey [7] and Remus [8] AUVs. Additional approaches to supplement these methods include novel applications of LBL [9] and vision-based navigation for very short-range homing [10]. Single-beacon navigation is used by the Hugin [11] and Theseus [12] AUVs to extend their LBL systems by incorporating ranges from a single beacon when necessary. And [13] reports use of an upward-looking Doppler velocity log (DVL) on the Gavia AUV for ice-relative navigation.

In this paper we report on a real-time acoustic navigation system developed for the Office of Naval Research (ONR) marginal ice zone (MIZ) program [14]. The ONR MIZ

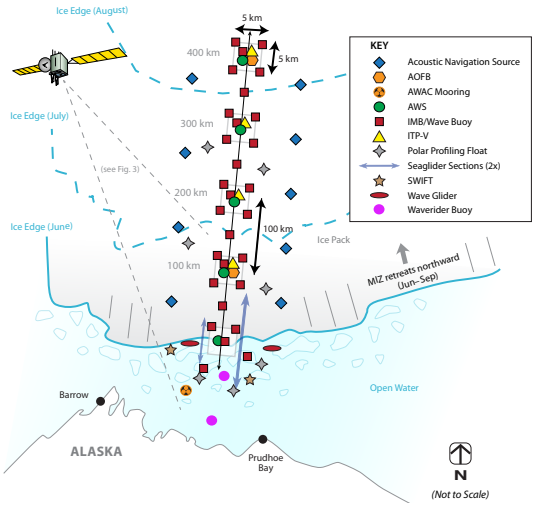

Fig. 1: Schematic of the marginal ice zone program field campaign [14]. Photo credit: APL-UW.

Postdoctoral funding for Sarah E. Webster was provided by ARC1022472 and N00014-12-G-0078. The development of ice-capable Seagliders, ongoing operations in Davis Strait, and operations in the Arctic in summer 2014 are supported by NSF OPP grants ARC1022472, ARC0632231, OPP0230381, ONR grants N00014-12-1-0180, N00014-12-G-0078, and N00014-12-I-0176 & N00014-12-I-0225 (WHOI).

program was designed to be an ice-based experiment, as shown in Fig. 1, as opposed to an ice breaker-based campaign or a subsurface mooring deployment. Because of this, the navigation sources could not be pre-deployed through the ice to rest on the seafloor. Otherwise, as the instrumented area of ice moved, the sources would not be in the correct position to support the AUGs making synoptic measurements with the sensors on the ice. In addition, because real-time position information was important for navigation of the AUGs, the time-of-flight measurements could not simply be saved and post-processed along with the known source locations (sent back via Iridium) after recovery. Instead the acoustic navigation sources were required to transmit their location so that the AUG could decoded and use it, thus motivating the design of a new generation of long-range, low-frequency navigation source: one that includes communications.

The concept of transmitting source location information along with timing data is not new; the global positioning system (GPS) signals include low-rate telemetry data, and the concept has been exploited for small underwater networks with mobile navigation sources, for example in [15], [16], [17], [18] and [19]. However, this is the first time that such an approach has been used in the Arctic to make a complete navigation system.

The remainder of this paper is organized as follows. The acoustic navigation beacons and receivers are described in Sec. II. The real-time navigation algorithm is described in detail in Sec. III. The MIZ field campaign is briefly described in Sec. IV, followed by results and discussion in Sec. V. We conclude in Sec. VI with lessons learned and future work.

II. Acoustic Navigation Beacons and Receivers

The acoustic beacons and receivers are based on the Micro-Modem 2, a newer version of the Micro-Modem which has been in development at the Woods Hole Oceanographic Institution for more than 15 years [20], [21] and used in many underwater navigation systems [22]. The beacons (Fig. 2) are fabricated so that they will float when the ice melts, and include GPS receiver, Iridium satellite communications, low-frequency amplifier, and 900 Hz flexural disk transducer. The receivers are simply a Micro-Modem 2 circuit board and an omni-directional hydrophone from High-Tech Inc. While the beacons use a GPS for timing, the timing reference on the Seagliders are SeaScan Inc. temperature-compensated oscillators. The receivers are low-power (< 0.5 W), and are turned off when no incoming navigation receptions are expected. Likewise, the buoy beacons are off except when a transmission is scheduled. The beacons were designed for a minimum of 6 months of use when transmitting every four hours, but if equipped with a larger battery pack could last much longer (unless crushed or covered by ice).

The carrier frequency is 900 Hz, signal bandwidth is 25 Hz (both FM sweep for navigation time and for data), and the data is encoded with a low-rate error-correction that results in a data rate of approximately 1 bps. The source level is

(a) Acoustic navigation buoy.

(b) Flexural disk transducer.

Fig. 2: Acoustic navigation buoy hardware. Initially deployed on the ice, the GPS- and Iridium-equipped buoy sits on the ice, while the acoustic transducer hangs below through a hole in the ice. The buoy is designed to survive the ice breakup. For the MIZ program, the transducers were at $\sim$105 m depth.

183 dB re micro-pascal, which requires less than 50 W of power from the battery.

The beacon transmission consists of a frequency-modulated sweep, followed by a short gap, then phase-modulated data. The frequency-modulated sweep is detected at the receiver and used for the time-of-arrival estimate, while the phase-modulated signal is processed using an adaptive equalizer with embedded error-correction decoding and Doppler compensation. The accuracy of the time-of-arrival estimate is a function of its bandwidth, the signal-to-noise ratio (SNR), and the channel response. Despite the modest bandwidth of B=25 Hz, if only one ray is present and the SNR is high, the accuracy can be on the order of a few meters or better. To take advantage of this, the peak of the matched-filter output (sampled at 2B) is interpolated to find the peak, and this travel time is reported to the navigation system.

The data payload contains one byte of destination address and up to 9 bytes of configurable payload. We have divided this into source position, command, and target position as shown in Table I, where the command and target positions are used to send the glider to a specific location. The decimated source latitude and longitude are created by scaling latitude by 5000 and longitude by 2500 and rounding to nearest integer, which results in 22 m resolution in latitude and 10 m resolution in longitude at 75^oN. Similarly, decimating the target latitude and longitude into 12 bits each results in a resolution of 5 km in latitude and 2.5 km in longitude at 75^oN, adequate for the purposes of this program.

Table II shows the schedule of acoustic broadcasts for one cycle of transmissions; the cycle was repeated at the top of every fourth hour. To avoid interference between the signals from different sources, each source transmits at the beginning of its own four-minute slot. The signal takes up approximately one minute, which allows for approximately 240 km of channel-clearing time. The use of staggered

transmissions results in range estimates made along a moving track and is one motivation for using a Kalman filter to properly integrate them into the navigation solution.

The receiver provides the time of arrival and packet data, including source position, to the AUG after the data are decoded. The AUG uses the source schedule to determine what minute the source transmitted and computes the one-way travel time. The transmissions are scheduled every four hours in this deployment, but that interval is programmable and can be changed if necessary depending on mission requirements.

III. Real-time Acoustic Navigation Algorithm

The acoustic navigation algorithm reported herein is a real-time implementation of the algorithm reported in [4], which is in turn based on the one-way-travel-time (OWTT) navigation algorithm reported in [15]. The real-time implementation, written in C, required a few modifications of the full 6 degree-of-freedom (DOF) model used in [4].

A. State Vector and Process Model

For the real-time filter, as in [4], we use a constant-velocity process model. However, because of the limited processing power currently available on Seaglider, we reduced the filter state to track only position and associated velocities in the world frame (North, East, down), as shown in (1). Position North and East are recorded in minutes of latitude and minutes of longitude, respectively, while depth is in meters and all velocities are in meters per second. Horizontal position is not stored in meters because the distances traversed by the AUG, and the distances between the AUG and the acoustic sources (hundreds of kilometers), make the use of a local origin impractical. However, because the navigation algorithm is implemented using single precision floating point numbers, numerical stability issues arose when converting between meters and degrees latitude or longitude in the state transition matrix. The use of minutes latitude and minutes longitude avoids this accuracy problem without resorting to the use of a local origin.

$$\boldsymbol{x} = \begin{bmatrix} x \\ y \\ z \\ \dot{x} \\ \dot{y} \\ \dot{z} \end{bmatrix} \begin{array}{l} \text{[minutes latitude]} \\ \text{[minutes longitude]} \\ \text{[meters depth]} \\ \text{[meters/second N]} \\ \text{[meters/second E]} \\ \text{[meters/second down]} \end{array} \tag{1}$$

When AUG attitude is required, e.g., for transforming body velocity estimates into the world frame, the most recent compass reading is used without filtering. This approach for a reduced-order model is a common simplification for real-time operations when attitude and depth are well-instrumented and have bounded error.

The reduced-order state vector and constant-velocity process model result in a nearly linear state transition matrix (2), shown here in discrete time, where m_{lat} and m_{lon} are meters per minute of latitude and longitude respectively.

$$\boldsymbol{x}_{k+1} = \begin{bmatrix} \boldsymbol{I} & \boldsymbol{F} \\ \boldsymbol{0} & \boldsymbol{I} \end{bmatrix} \boldsymbol{x}_k \tag{2}$$

$$\boldsymbol{F} = \begin{bmatrix} \Delta t/m_{lat} & 0 & 0 \\ 0 & \Delta t/m_{lon} & 0 \\ 0 & 0 & \Delta t \end{bmatrix}$$

Note that m_{lat} is constant, but m_{lon} varies with the cosine of latitude. This cosine prevents the process model from being strictly linear. However, in practice the latitude changes so slowly with each timestep that we are able to treat this term as constant for each prediction step. As a result, we avoid a computationally costly linearization at each prediction step, compared to the 6 DOF model. Even more importantly from a computational standpoint, this enables us to perform a single prediction between measurements regardless of the size of the time step. This is in contrast to the nonlinear process model reported in [15], which requires a limit on the maximum length of a single prediction step to prevent large linearization errors, thus requiring multiple prediction steps to advance the filter state up to the time of the next measurement.

The use of a single prediction step between measurements is especially important for Seaglider operations because of the paucity of sensor measurements compared to traditional AUVs. As shown in Table III, up to 30 seconds elapses between sensor measurements while the AUG is diving, and often a *minimum* of 5 minutes elapses between the two GPS

TABLE I: Breakdown of 72-bit acoustic packet payload.

# of Bits	Use	Resolution
20	source lat	22 m
20	source lon	10 m (at 75^{o}N)
8	command	n/a
12	target lat	5 km
12	target lon	2.5 km (at 75^{o}N)
72	**Total**	

TABLE II: Acoustic source broadcast schedule (repeated every 4 hours).

Source ID	Broadcast Time	Source ID	Broadcast Time
1	0:00	8	0:24
2	0:04	9	0:30
4	0:08	10	0:34
5	0:12	13*	0:38
6	0:16	14*	0:42
7	0:20		

*Mobile acoustic sources mounted on Wave Gliders at 4.5 m depth.

TABLE III: Typical Seaglider sampling schedule.

Vehicle Depth	Frequency	Sensor Measurement
surface	twice per dive	GPS
5–250 m	every 10 sec	pressure, roll, pitch, heading, and estimated velocity (from pitch and buoyancy)
250–1000 m	every 30 sec	
any depth	every 4 hours	acoustic broadcast from each source

fixes on the surface, during which time no other sensor measurements are available.

B. On-Board Sensor Measurements

Seaglider AUGs carry a minimal sensor suite for navigation. The Seagliders deployed during the experiments described herein carried only a Sparton compass (SP3004D), a Paine pressure sensor (Model 211-75-710-05, a strain gauge sensor with 1500 psi full-scale range and 0.25% FS accuracy), a Garmin GPS sensor (GPS-15xH), and the navigation receiver described above. The uncertainties assigned to each observation model are shown in Table IV.

TABLE IV: Seaglider navigation sensor model uncertainties.

Measurement (Sensor)	State	Uncertainty
pressure (Paine)	z	0.5 m
velocity (buoyancy & pitch)†	$\dot{x}, \dot{y}$	0.06 cm/s
acoustic range	x, y	4.0*(range in km) m‡

† The Seaglider hydrodynamic model uses pitch and either buoyancy or vertical velocity to predict angle of attack and forward velocity.
‡ We also set a minimum uncertainty of 50 m.

To provide a sense of velocity through the water, we use the Seaglider hydrodynamic model. Described in detail in [23], the lift and drag model parameters are tuned for each Seaglider after deployment in order to provide an estimate of forward velocity and the angle of attack based on pitch and either vertical velocity or buoyancy. The resulting velocity estimate is incorporated into the filter as a measurement.

While it may seem indirect to treat the hydrodynamic model output as a measurement, as opposed to using the hydrodynamic model as the process model for the filter, there are two reasons that we do this. First, the hydrodynamic model is not used as the AUG process model because it is highly nonlinear and would require linearization with each prediction step, imposing the limitations described in Sec III-A. Second, the hydrodynamic model is used within the Seaglider software to estimate velocity whenever a compass reading is taken regardless of what navigation algorithm is running. Therefore it saves processing time to use the output of that function call as velocity pseudo-measurements instead of calling the hydrodynamic model function again for each prediction step.

C. Acoustic Range Estimates

The range between an acoustic navigation source and the AUG is estimated using the time-of-flight of the acoustic message broadcast. As described in [24], we can treat these range measurements as independent and uncorrelated because the acoustic source positions are based on GPS measurements. The uncertainty assigned to the acoustic range observation model was determined experimentally using the range innovations to tune the Kalman filter. A range-dependent error model is employed because of the expected effect of ray bending, compounded by long distances, when the receiver (the AUG) is at a significantly different depth from the source. As reported in Table IV, we found an uncertainty of 4.0 m per km of range produced consistent filter results.

Calculating the AUG's range from the sources based on the one-way travel time requires synchronized clocks on the sources and the AUGs and assumptions about sound speed and ray bending. Navigation source clocks receive a pulse-per-second (PPS) signal directly from GPS. Seascan Inc. clocks are used onboard Seagliders for a stable reference and these are disciplined with every GPS fix. With a drift rate of 0.001 second/day, 10 days under ice without a GPS fix would result in only 15 m of error in range. The local sound speed at the AUG at the time of reception is used to estimate range from time-of-flight. While not optimal, we have not yet developed a method for estimating the sound-speed along the path from source and receiver by taking advantage of *in situ* measurements and climatology.

D. Under-Ice Current Estimates from the AUG

Most AUGs provide an estimate of depth-averaged current (DAC) based on the difference between their estimated dead-reckoned surfacing position and their actual surfacing position (from a GPS measurement). AUGs are able to use this estimated DAC to account for current-induced set and drift and adjust the desired heading for the next dive accordingly, resulting in straighter tracklines and more headway toward the desired target. One of the unique contributions of the navigation algorithm presented herein is the addition of an average current calculation based only on range measurements, that can be made while the AUG is under ice without access to GPS.

Within the Kalman filter framework, the standard DAC can be found by dividing the GPS measurement innovation by the time since the previous GPS measurement. As part of the real-time algorithm, we implemented a method to estimate range-based averaged currents (RACs), which represent the average current experienced by the vehicle between cycles of range measurements. Because the acoustic broadcasts are tightly grouped, a local minimum of uncertainty in vehicle position is achieved at the end of each cycle of transmissions. To estimate the effect of current on the vehicle's trajectory between local minimums, the algorithm keeps a cumulative sum of the x- and y-components of the range innovations during each cycle of transmissions. At the end of each cycle, the cumulative innovation is divided by the elapsed time since the last RAC calculation (at the end of the previous cycle of transmissions) to estimate the new RAC.

Unlike DAC estimates, RAC estimates do not represent a full depth-averaged current because the vehicle traverses variable portions of the depth profile between each cycle of range measurements. The extent of the depth profile that is traversed is not knowable *a priori* because it depends on the real-time operation of the vehicle compared to the timing of the broadcasts. As a result, the RACs may not be a suitable substitute for DACs for navigation purposes in strongly vertically stratified currents without taking the vehicle depth trajectory into account.

The fidelity of the RAC estimates are highly dependent on the quantity and accuracy of the range measurements, because these determine the uncertainty of the vehicle's

starting and ending positions. If the cumulative uncertainty divided by the time is too large, the RAC estimate cannot be differentiated from noise. Given suitably accurate range measurements, however, with good throughput (where 'good' depends on the sensor suite and the deployment), we believe that this method could provide similar capability to the DAC estimate for real-time set and drift correction without requiring access to the surface.

IV. Marginal Ice Zone Field Campaign

The marginal ice zone field campaign ([14]) began in March when a small subset of the research team mobilized in Sachs Harbor, AK. All of the ice-based assets were deployed by plane, setting up camps on the ice as necessary. The science instruments were placed near 137^{o}W, grouped into four clusters spaced approximately 1.0^o latitude apart, from 72.5^{o}N to 75.5^{o}N. The acoustic navigation sources were placed in two rows on either side of the line of instrument clusters, to provide optimal acoustic coverage while the Seagliders transit near the clusters (see Fig. 1).

At the end of July, another team mobilized in Prudhoe Bay, AK, to deploy the mobile assets by small boat—four Seagliders, two Wave Gliders carrying acoustic navigation sources, two SWIFT buoys, and a WaveRider mooring. Once deployed the Seagliders and Wave Gliders moved north towards the array—the Wave Gliders providing acoustic navigation while staying clear of the ice, the Seagliders transiting under the ice and ice-fast instruments.

Figure 3 shows the evolution of the ice pack during the seasonal melt from April through September 2014, and the movement of the ice-fast and mobile assets deployed as part of the MIZ field program. The Seaglider campaign finished in early October when they were recovered after swimming south out of the reforming ice.

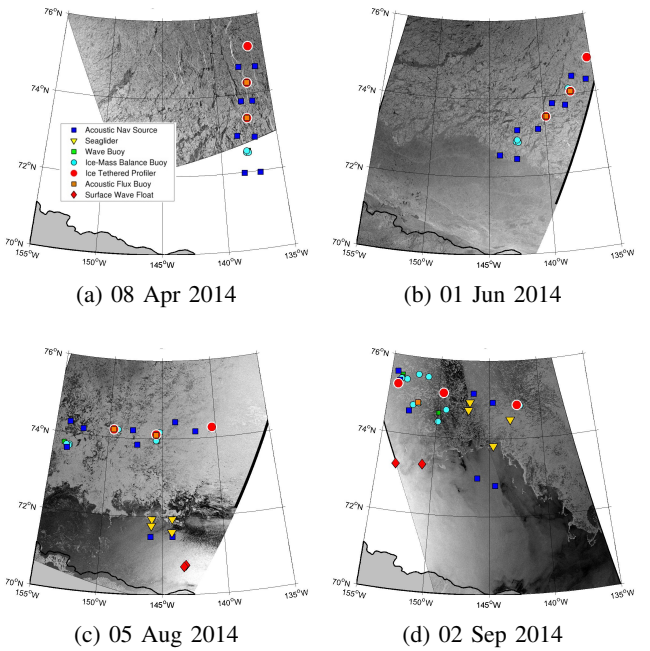

(a) 08 Apr 2014 (b) 01 Jun 2014

(c) 05 Aug 2014 (d) 02 Sep 2014

Fig. 3: Progression of the instrument array deployed north of Alaska, with satellite imagery underlayed when available. This shows the extreme deformation of the array of instruments, including the acoustic navigation beacons (blue squares) and the Seaglider deployments (yellow triangles). (a) Initial deployment of ice-based instrumentation. (b) Deformation of array after seven weeks. (c) Four Seagliders, two Wave Gliders with acoustic beacons (blue squares), and two SWIFT buoys (red diamonds) are deployed in open water south of the array. (d) Seagliders sample under the ice 15 days before the 2014 sea ice minimum.

V. Results and Discussion

In this section we summarize the performance of the travel time estimates made from transmissions between pairs of beacons, and from the beacons to the Seagliders. We also show results from the real-time navigation algorithm and current estimation using acoustic ranges.

A. Beacon-to-Beacon Performance

The receivers on each of the buoys are enabled during the entire period when they transmit, and thus we were able to monitor the performance of the system as soon as the network was deployed in late March. While the original plan for positioning was based on maximum ranges of approximately 100 km, it soon became clear that the system was operating at three times that estimate. Ice-tethered profilers [25] that were deployed at the same time showed the reason: a strong duct was present between 50 and 250 meters due to warm Pacific water above (at 50 m), and warm Atlantic water below (Fig. 4). The upper layer of the duct prevents the signal from interacting with the ice, where it would scatter, and the lower layer also refracts the signal back into the duct without loss. The presence of this duct was anticipated based

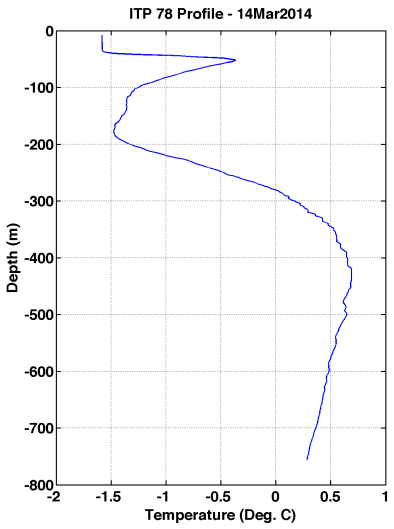

Fig. 4: Temperature versus depth in the central Beaufort in March when the buoys and other fixed sensors were deployed. This profile results in a sound channel between approximately 50 and 250 m.

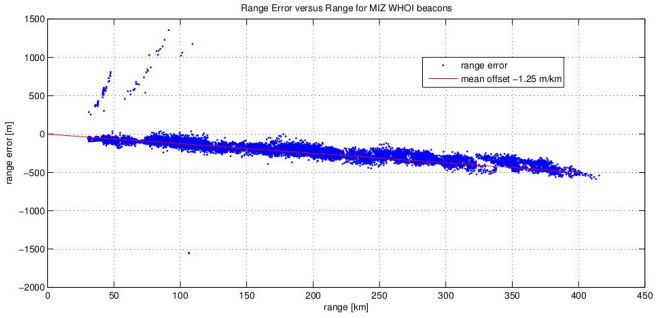

Fig. 5: Error in acoustic range estimates versus range between the ice-tethered acoustic navigation sources located in the sound channel, assuming a sound speed of 1437.2. The red line represents a range dependent offset of -1.25 meters per kilometer of range, which can be removed by adjusting the sound speed. Note that the precision is not range-dependent.

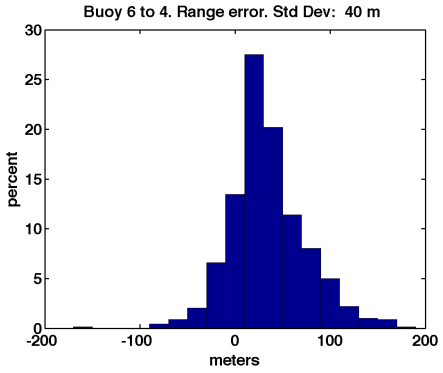

Fig. 6: Histogram of the error in the acoustic range estimates between sources 4 and 6 after adjusting the sound speed.

on the analysis of historic data, which informed the beacon transducer placement at 105 m depth, but the strength of the sound channel was not.

Additional key features of the duct are that it is stable and has similar shape throughout the Canada Basin; and that it is narrow, which results in minimal time spread of the wavefront. As a result the range estimate errors, made by comparing the measured travel times versus the ranges computed from the GPS positions, are independent of range, as shown in Fig. 5. The standard deviation of range error computed for one source-receiver pair (buoy 6 to 4) at approximately 200-250 km range was 40 m (Fig. 6). The success rate (percentage of the receptions that were detected acoustically and that were decoded successfully) was typically greater than 95%.

B. Beacon-to-Seaglider Performance

While the beacon-to-beacon transmissions were made in the duct, the Seagliders, by nature of their buoyancy-driven propulsion, were only in the duct a fraction of the time and not necessarily during a transmission window. Thus the performance of the receivers mounted on the Seagliders did not achieve the excellent range performance of the beacon receivers. However, the following observations may be made.

- For ranges less than approximately 100 km, the original design criterion of the navigation system, the Seagliders routinely heard the beacons and approximately half the time successfully decoded the source position data transmitted with it.
- At ranges from 100 to 300 km when receptions were made between the surface and 200 m depth, the majority of the detections resulted in good source locations.
- From 300 to 450 km the receptions with travel times that were deemed correct based on their arrival time very rarely had good associated source locations.

The reasons for the difference in performance are most likely due to propagation conditions in and out of the duct. Receivers in the duct hear the source at any range, while those outside the duct are in a range-dependent environment where signals come and go depending on the ray paths.

C. Navigation Algorithm Performance

The navigation algorithm ran on the Seagliders, in real-time, for the first ∼70 dives of each of the four deployed vehicles. Due to outside circumstances, real-time results from this algorithm are not available for the remainder of the deployment. The results presented herein are from post-processed analysis, however they use only the data that was available in real-time—raw navigation data and only the acoustic transmissions that were successfully decoded by the AUG in real time.

Figure 7 shows the filtered vehicle trajectory of sg198 for dives 193 to 272, a 295-hour segment during which the AUG successfully decoded 58 acoustic navigation packets. For comparison the dead-reckoned trajectory is shown in blue, for which GPS fixes were allowed but no range estimates were used. GPS fixes are shown in black.

Figure 8 shows the range measurement innovations for the same segment, color coded by acoustic source, with the 3-sigma measurement covariance limits shown in dashed magenta. The innovations for most of the sources lie within the 3-sigma bounds, indicating consistent measurements. Source 6, however, is clearly outside of the covariance bounds, with innovations around 15 km. The exact nature of the error is still under investigation, but possible causes are ray bending compounded by long ranges (∼ 450 km) and variability in the surface ice or clock drift/offset.

D. Under-Ice Current Estimates

As described in Sec. III-D, it is difficult to quantitatively compare RAC and DAC estimates without an external ground truth, and the fidelity of the RAC estimates are directly affected by the position uncertainty in the vehicle trajectory.

By design, the sources for the MIZ experiment were placed hundreds of kilometers apart to provide coverage over a large area. In the initial deployment the sources spanned 379 km, which spread to 461 km by the time the Seagliders were deployed, and continued to spread from there. As a result, range measurements from the MIZ experiment are too sparse to reliably compute RAC estimates, because the

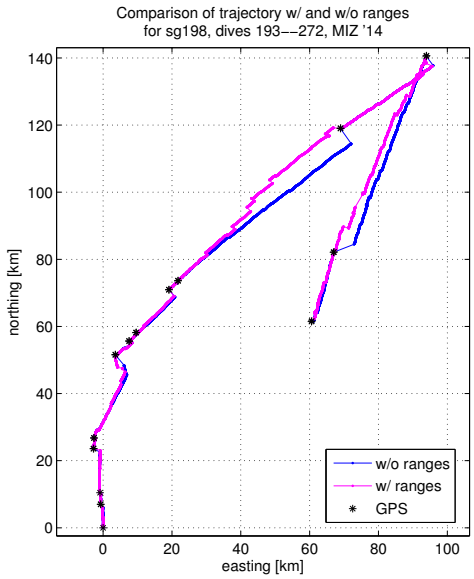

Fig. 7: Comparison of the dead-reckoned versus range-aided trajectory of sg198 during a 295-hour segment with some portions under the ice.

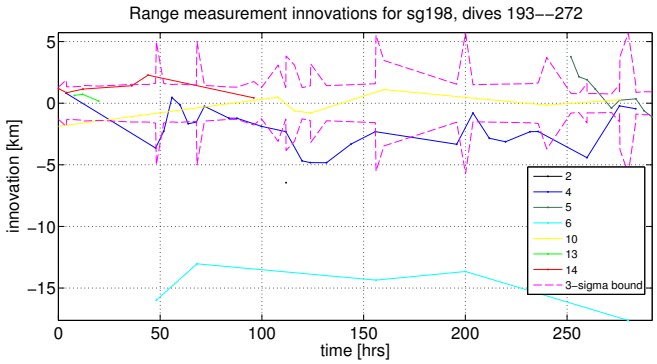

Fig. 8: Range innovations with the 3-sigma covariance bound for the 58 acoustic navigation packets decoded in real-time during the 295-hour segment shown in Fig 7. Innovations are color coded by source.

Seagliders rarely received more than one or two range measurements per cycle.

Instead, we will illustrate RAC estimation using data from a previous Seaglider deployment in Davis Strait. In Davis Strait, seven acoustic sources were deployed across 140 km, with a transmission cycle of 6 hours [4]. During each cycle, the Seaglider often receives a minimum of three range estimates. Figure 9 shows a comparison of range-average current estimates and depth-averaged current estimates from a section in 2011 where the vehicle was under ice with only periodic surfacings. Estimates are plotted as a stair step, such that the current shown at any given time is the current that was calculated at end of the previous cycle.

The caveat in this analysis is the that the range estimates in Davis Strait have significant uncertainty, 1.5–3 km, such that a typical 3-sigma position uncertainty after a transmission cycle could be up to 500 m. With that magnitude uncertainty

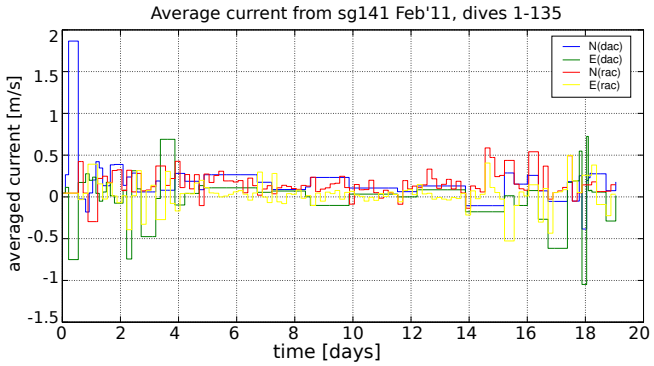

Fig. 9: Stairstep plots of North and East components of the average current calculated on a per-dive basis when GPS is available (DAC) versus after each cycle of range estimates (RAC). The lack of GPS measurements results in the DAC not being updated as often as the RAC; the large DAC after the first dive is a processing artifact.

on either end of a 6 hours dive, any current estimates less than 5 cm/s are undifferentiable from noise. Thus, without better data or ground truth for comparison, we do not yet make any quantitative claims about the RAC estimates. This comparison does show, however, that the RAC estimates are both larger than what we estimate to be noise, and are within reasonable bounds for typical currents in Davis Strait.

VI. Lessons Learned and Future Work

We described herein the design of a real-time, under-ice, mesoscale acoustic navigation system, including new hardware and a navigation algorithm that, in addition to vehicle position, is capable of estimating average subsea currents from acoustic range estimates when GPS fixes are unavailable. We presented initial experimental results from a deployment of the navigation system and four Seaglider AUGs in the marginal ice zone of the Beaufort Sea during the 2014 seasonal summer ice melt.

The acoustic navigation beacons provided reliable acoustic range estimates and data transfer to the AUGs throughout the water column out to 100 km with approximately 50% throughput. Range estimates and data transfer within the sounds channel (50–200 m) were reliable out to 300 km with occasional receptions out to 450 km.

Post-processed results from the navigation algorithm show that it is effective in both estimating vehicle position and produces average current estimates that are consistent in magnitude with depth-averaged currents, given adequate range data.

Several operational lessons were learned from this field program. First, the strong acoustic channel significantly degraded the throughput of acoustic navigation packets when the AUGs were outside of the sound channel. Coordinating acoustic transmissions and the AUG residence in the sound channel should improve throughput. Second, in post-processing we were able to infer the source of many of the transmissions when the data packet was not successfully

decoded. For the dives analysed here, this would have added 25 range hits to the original 58. Adding this logic and a simple filter to predict source locations could provide useful range data at longer distances, especially in the absence of proper range hits. Finally, a clock problem on one of the AUGs rendered real-time acoustic navigation unusable. Diagnosing clock problems automatically would not be difficult, so implementing a back-up strategy would be advantageous, especially for long missions under the ice.

Additional future work includes additional analysis of the navigation and science data from the MIZ experiment. We are reporting very early results from the MIZ field campaign. As such there is much yet to learn about the marginal ice zone and its acoustic environment. Using both Seaglider conductivity and temperature data and similar data from ice-tethered profilers deployed as part of the MIZ field campaign, we can better estimate the sound speed profile in the marginal ice zone. This will enable us to better characterize the average sound velocity, the effects of ray-bending, and how best to estimate these onboard the AUG in real-time for more accurate range estimates. For the navigation algorithm, we intend to investigate the usefulness of including a clock offset for individual sources within the filter to improve performance. In addition, we look forward to continuing to develop and test the capability of estimating average currents subsea from range measurements.

ACKNOWLEDGMENTS

The development of ice-capable Seagliders and on-going operations in Davis Strait, and the MIZ program were made possible with the help of Geoff Shilling, Luc Rainville, Beth Curry, Adam Huxtable, Ben Jokinen, Keith Van Thiel, Eric Boget, Kunuk Lennert and the crew of F/V Nanna, Captain Sheasley and the crew of R/V Knorr, and Captain Rink and the crew of R/V Sanna. The acoustic navigation system development team at WHOI included Jim Partan, Sandipa Singh, Keenan Ball, Andrew Beal and Peter Koski.

REFERENCES

[1] R. Francois and W. Nodland, "Unmanned Arctic research submersible (UARS) system development and test report." APL-UW, Washington, Report 7219:87, 1972.

[2] "Study of Environmental Arctic Change (SEARCH), 2005: *Study of Environmental Arctic Change: Plans for implementation during the International Polar Year and beyond.*" Fairbanks, Alaska, 2005, pp. 104. [Online]. Available: http://www.arcus.org/files/page/documents/19092/siw_report_final.pdf

[3] "ANCHOR group, 2007. *Acoustic Navigation and Communications for High-latitude Ocean Research: A Report from an International Workshop Sponsored by the National Science Foundation Office of Polar Programs*," Seattle, WA, 27 February–1 March 2006, pp. 55. [Online]. Available: http://anchor.apl.washington.edu/ANCHOR_workshop_report.pdf

[4] S. E. Webster, C. M. Lee, and J. I. Gobat, "Preliminary results in under-ice acoustic navigation for Seagliders in Davis Strait," in *Proc. IEEE/MTS OCEANS Conf. Exhib.*, St. John's, Newfoundland, Sept. 2014, pp. 1–5.

[5] T. Rossby, D. Dorson, and J. Fontaine, "The RAFOS System," *Journal of Atmospheric and Oceanic Technology*, vol. 3, pp. 672–679, 1986.

[6] C. Jones, B. Allsup, and C. DeCollibus, "Slocum glider: Expanding our understanding of the oceans," in *Proc. IEEE/MTS OCEANS Conf. Exhib.*, St. John's, Newfoundland, Sept. 2014, pp. 1–10.

[7] M. Deffenbaugh, H. Schmidt, and J. Bellingham, "Acoustic navigation for Arctic under-ice AUV missions," in *Proc. IEEE/MTS OCEANS Conf. Exhib.*, vol. 1, Victoria, BC, Oct. 1993, pp. 1204–1209.

[8] A. Kukulya, A. Plueddemann, T. Austin, R. Stokey, M. Purcell, B. Allen, R. Littlefield, L. Freitag, P. Koski, E. Gallimore, J. Kemp, K. Newhall, and J. Pietro, "Under-ice operations with a REMUS-100 AUV in the Arctic," in *IEEE/OES Auto. Und. Veh. (AUV)*, Sept. 2010, pp. 1–8.

[9] M. V. Jakuba, C. N. Roman, H. Singh, C. Murphy, C. Kunz, C. Willis, T. Sato, and R. A. Sohn, "Long-baseline acoustic navigation for under-ice autonomous underwater vehicle operations." *J. Field Rob.*, vol. 25, pp. 861–879, 2008.

[10] M. Hildebrandt, J. Albiez, M. Fritsche, J. Hilljegerdes, P. Kloss, M. Wirtz, and F. Kirchner, "Design of an autonomous under-ice exploration system," in *Proc. IEEE/MTS OCEANS Conf. Exhib.*, San Diego, CA, Sept. 2013, pp. 1–6.

[11] O. Hegrenaes, K. Gade, O. Hagen, and P. Hagen, "Underwater transponder positioning and navigation of autonomous underwater vehicles," in *Proc. IEEE/MTS OCEANS Conf. Exhib.*, Biloxi, MS, Oct. 2009, pp. 1–7.

[12] C. Kaminski, T. Crees, J. Ferguson, A. Forrest, J. Williams, D. Hopkin, and G. Heard, "12 days under ice — an historic AUV deployment in the Canadian High Arctic," in *IEEE/OES Auto. Und. Veh. (AUV)*, Sept. 2010, pp. 1–11.

[13] M. Doble, P. Wadhams, A. Forrest, and B. Laval, "Experiences from two-years' through-ice AUV deployments in the High Arctic," in *IEEE/OES Auto. Und. Veh. (AUV)*, Oct. 2008, pp. 1–7.

[14] C. Lee, S. Cole, M. Doble, L. Freitag, P. Hwang, S. Jayne, M. Jeffries, R. Krishfield, T. Maksym, W. Maslowski, B. Owens, P. Posey, L. Rainville, B. Shaw, T. Stanton, J. Thomson, M.-L. Timmermansan, J. Toole, P. Wadhams, J. Wilkinson, and Z. Zhang, "Marginal ice zone (miz) program: Science and experiment plan," Applied Physics Laboratory, University of Washington, Seattle, WA, Technical Report APL-UW 1201, September 2012, 48 pp.

[15] S. E. Webster, R. M. Eustice, H. Singh, and L. L. Whitcomb, "Advances in single-beacon one-way-travel-time acoustic navigation for underwater vehicles," *Intl. J. Robot. Res.*, vol. 31, no. 8, pp. 935–950, July 2012.

[16] J. M. Walls and R. M. Eustice, "An origin state method for communication constrained cooperative localization with robustness to packet loss," *Intl. J. Robot. Res.*, vol. 33, no. 9, pp. 1191–1208, 2014.

[17] A. Bahr, M. Walter, and J. Leonard, "Consistent cooperative localization," in *Proc. IEEE Intl. Conf. Robot. Auto. (ICRA)*, Kobe, Japan, May 2009, pp. 3415–3422.

[18] M. F. Fallon, G. Papadopoulos, J. J. Leonard, and N. M. Patrikalakis, "Cooperative AUV navigation using a single maneuvering surface craft," *Intl. J. Robot. Res.*, vol. 29, no. 12, pp. 1461–1474, Oct. 2010.

[19] J. Vaganay, J. Leonard, J. Curcio, and J. Willcox, "Experimental validation of the moving long base-line navigation concept," in *IEEE/OES Auto. Und. Veh. (AUV)*, June 2004, pp. 59–65.

[20] L. Freitag, M. Grund, S. Singh, J. Partan, P. Koski, and K. Ball, "The WHOI Micro-Modem: an acoustic communications and navigation system for multiple platforms," in *Proc. IEEE/MTS OCEANS Conf. Exhib.*, Washington, D.C., Sept. 2005, pp. 1086–1092.

[21] E. Gallimore, J. Partan, I. Vaughn, S. Singh, J. Shusta, and L. Freitag, "The WHOI Micro-Modem-2: A scalable system for acoustic communications and networking," in *Proc. IEEE/MTS OCEANS Conf. Exhib.*, Seattle, WA, Sept. 2010, pp. 1–7.

[22] S. Singh, M. Grund, B. Bingham, R. M. Eustice, H. Singh, and L. Freitag, "Underwater acoustic navigation with the WHOI Micro-Modem," in *Proc. IEEE/MTS OCEANS Conf. Exhib.*, Boston, MA, Sept. 2006, pp. 1–4.

[23] C. C. Eriksen, T. J. Osse, R. D. Light, T. Wen, T. W. Lehman, P. L. Sabin, J. W. Ballard, and A. M. Chiodi, "Seaglider: A long-range autonomous underwater vehicle for oceanographic research," *IEEE J. Oceanic Eng.*, vol. 26, pp. 424–436, Oct. 2001.

[24] J. M. Walls and R. M. Eustice, "Experimental comparison of synchronous-clock cooperative acoustic navigation algorithms," in *Proc. IEEE/MTS OCEANS Conf. Exhib.*, Kona, HI, Sept. 2011, pp. 1–7.

[25] S. T. Cole, M.-L. Timmermans, J. M. Toole, R. A. Krishfield, and F. T. Thwaites, "Ekman veering, internal waves, and turbulence observed under arctic sea ice," *J. Phys. Oceanogr.*, vol. 44, pp. 1306–1328, 2014.